Adhesion of cylindrical colloids to the surface of a membrane

Sergey Mkrtchyan, Christopher Ing, and Jeff Z. Y. Chen
Department of Physics and Astronomy, University of Waterloo, Waterloo, Ontario, Canada N2L 3G1
(Received 12 June 2009; revised manuscript received 20 November 2009; published 12 January 2010)

We study the system of cylindrical colloids adhering to an originally flat fluid membrane, on the basis of a full treatment of the Helfrich model. Our approach allows for numerical calculation of the free energy in both shallow- and deep-wrapping conformations. We show that the free energy of two cylinders adhering to the same side of a membrane has two branches corresponding to shallow and deep wrapping and that the system of two cylinders adhering to opposite sides of a membrane can undergo a first-order phase transition between two membrane-mediated attractive states.

DOI: 10.1103/PhysRevE.81.011904 PACS number(s): 87.16.dt, 87.15.kt, 81.07.−b

I. INTRODUCTION

Recent theoretical studies and computer simulations of simple models, involving interactions between a membrane and macromolecules including polymers and nanosized colloid particles, have demonstrated the existence of a variety of interesting structures and complex phase behavior. For example, now we know that the curvature around either polymer-tethering, polymer-adsorbing, or rod-adsorbing region of a membrane is expected to be significantly modified [1–9]; the interaction between a bulk of nanoparticles and a membrane surface can create a curvature on the membrane [10]; the adhering nanoparticles between two membrane sheets can produce mediate attraction between membranes [11,12]; the adhesion of a single nanoparticle with relatively large dimension on a membrane can produce a deep engulfing of the membrane sheet on the particle [13,14] and this is similar to the budding transition seen in numerical simulations [15,16]; a pearling instability exists when a hollow tubular vesicle interacts with a polymer solution [17]; a swollen-to-globular transition of a polymer confined in a tubular membrane can be induced when the tension on the membrane changes [18,19]; adsorbed colloid particles on a flat membrane sheet or colloid particles confined in a tubular membrane may experience membrane-mediated force between the particles [20–22]. These structural and dynamical understanding provide enlightening explanation of real biological systems where the interactions between surfaces and macromolecules are common.

In most theoretical treatment, a phospholipid bilayer membrane is approximated by a soft, bendable sheet with negligible thickness, which will be done in this article as well. At this level of approximation, the physical nature of fluid membranes and vesicles can be well captured by the Helfrich model [23,24], which is now usually used as a theoretical basis for understanding the conformational and dynamical properties of membrane-related systems [25,26]. Within the theoretical framework of the Helfrich energy and after the introduction of an additional phenomenological parameter, adhesion energy per unit area, Deserno and coworkers examined the system of an originally flat fluid membrane interacting with a single *spherical* colloid particle. Even in such a simple system, as the adhesion energy or the membrane tension change, two stages of phase transition can occur: a second-order adsorption transition where the sphere starts to bind a weakly deformed membrane and a first-order partial-to-full wrapping transition where the last phase contains an almost fully wrapped sphere with a highly deformed membrane shape [13,14,27].

Another even simpler but also illustrative system is a flat membrane interacting with *cylindrical* colloid particles. Boulbitch determined a binding transition [28] between a single cylinder and membrane [see illustration in Fig. 1(A)], through an analysis of the free energy of the system. When two colloid particles are adhered to a common fluid membrane surface, the competitive adhesion energy and membrane deformation energy stabilize the conformation of the entire system [see illustrations in Figs. 1(B) and 1(C)]. As a basic model we can assume that the colloid particles have negligible interactions between themselves; membrane-mediated interactions between these adhered particles become an interesting physical phenomenon [20], as was recently visited by Muller, Deserno and Guven in a general theoretical framework [21,29]. The theoretical problem of membrane-mediated interaction between two *cylinders* adhering to the same and opposite sides of a membrane was previously studied in detail in Ref. [20], where the shape profile was described in terms of small deviations of the membrane surface from a flat reference plane. Although being accurate for small membrane deformations this approach does not take significant overhangs into account, where cyl-

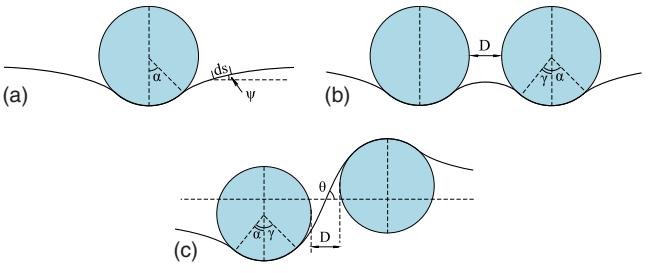

FIG. 1. (Color online) Sketch of the cross section of three systems considered. The curves represent a cross-section view of the membrane profile. Plot (a) shows a single cylinder adhered to a membrane, where the wrapping angle α and tangent angle ψ are also defined. Plots (b) and (c) show two cylinders adhered to a membrane, where the surface-to-surface distance D, wrapping angle γ, and crossing angle θ are also specified.

inders can possibly become deeply wrapped by the membrane.

In biological systems, a family of protein modules known as BAR domains are able to bind lipid membranes and the binding induces tubular membrane structures. Experiments show that different types of protein domains curve membrane differently which results in different sizes of tubules. This can be used to control the size of the transported particles in membrane trafficking [30,31].

In this paper, we present a treatment of the problem in terms of a full consideration of the Helfrich free energy, without the small-displacement expansion taken in Refs. [20,28]. As described in Sec. II, because of the embedded symmetry in the system, in a cross-section view [see, e.g., Fig. 1(A)], the membrane shape can be represented by a curve, where the dimension along the cylinder axis can be suppressed, effectively yielding a two-dimensional problem. Using the tangent angle ψ of the curve as the variable, we show below that the formalism allows us to directly write down the free energy of the entire system, minimization of which yielding the stable structure. In Sec. III, we revisit the problem of single cylinder adhesion to a membrane surface, laying down the groundwork for Sec. IV where the adhesion of two cylinders to the same side of a membrane surface is discussed and Sec. V where the adhesion of two cylinders to the opposite sides of a membrane surface is discussed. In the parameter regime where small variations of the membrane shape are seen, we recover previous results in Refs. [20,28]; in the parameter region where the small-displacement expansion approximation is no longer valid, we obtain new structural conformations as discussed in these sections. Most results in this work are consistent with those drawn in Ref. [21] for the same system, where the stress force in these systems has been the main focus of the theoretical derivation.

II. MODEL

We use the coordinate system in Fig. 1(A), where a cross section of the cylinder-membrane system is shown. The variation of the membrane shape in the direction perpendicular to the plane shown is completely ignored, and the system becomes two-dimensional effectively. The membrane shape can then be described by the tangent angle $\psi(s)$ which is a function of the contour variable s. For the free section of the membrane we can write the Helfrich free energy [24] in a simple form,

$$F = \int \left[\frac{1}{2}\kappa \left(\frac{d\psi}{ds} \right)^2 + \sigma \right] L ds, \tag{1}$$

where κ is the bending energy, σ the surface tension, and L the length of the system along the cylinder axis. Long cylinders $L \gg R$ are assumed where R is the adhering cylinder radius and the end effects are ignored in this article. Subtracting the free energy of a freely standing, planar membrane and introducing dimensionless quantities,

$$\tilde{F} = FR/\kappa L, \tag{2}$$

$$\tilde{\sigma} = \sigma R^2/\kappa, \tag{3}$$

$$\tilde{s} = s/R, \tag{4}$$

we obtain a reduced free energy difference,

$$\Delta \tilde{F} = \int \left[\frac{1}{2}\left(\frac{d\psi}{d\tilde{s}} \right)^2 + \tilde{\sigma}(1 - \cos\psi) \right] d\tilde{s}, \tag{5}$$

to be minimized with respect to the shape function $\psi(\tilde{s})$. The functional in the square brackets above can be regarded as a Lagrangian in a classical-dynamics formalism. The use of the Euler-Lagrange equation, for the $\psi(\tilde{s})$ minimizing the above free energy yields a second-order differential equation for $\psi(\tilde{s})$,

$$\frac{d^2\psi}{d\tilde{s}^2} - \tilde{\sigma} \sin\psi = 0. \tag{6}$$

A first integral, which corresponds to the Hamiltonian related to that Lagrangian, exists,

$$\frac{1}{2}\left(\frac{d\psi}{d\tilde{s}} \right)^2 - \tilde{\sigma}(1 - \cos\psi) = H, \tag{7}$$

where H is a constant. The first integral together with the free energy difference, Eq. (5), form the theoretical framework for deducing the free energy of considered systems below.

Muller, Deserno and Guven have arrived at the same equations [Eqs. (6) and (7)] from a consideration of balancing force in the system [21]. Consider a line parallel to the cylinder axis on the membrane that divides the membrane to the left and right sections. At this point one can define a force acting on the left section from the right section of the membrane. Projections on the directions, along the normal and parallel to the surface of the membrane, of this static force give rise to these two basic equations; however, only one of them is independent.

III. ADHESION OF A SINGLE CYLINDER TO A MEMBRANE

In this section we discuss the adsorption of a single cylinder to a membrane surface. The adsorbed portion of the membrane wraps around the cylinder with a wrapping angle α [see Fig. 1(A)], where an adhesion energy per unit area $-w$ is assumed. Because the membrane in the system is asymptotically flat at $\tilde{s}=\infty$ where $d\psi/d\tilde{s}=\psi=0$, the integration constant in Eq. (7) $H=0$. This leads to

$$\left(\frac{d\psi}{d\tilde{s}} \right)^2 = 2\tilde{\sigma}(1 - \cos\psi). \tag{8}$$

Using Eq. (8) in Eq. (5) we obtain the free energy difference for the free part of the membrane on both left and right sides

$$\Delta \tilde{F}_{\text{free}} = 2\int_0^\infty [2\tilde{\sigma}(1 - \cos\psi)] d\tilde{s}$$

$$= \sqrt{8\tilde{\sigma}} \int_0^\alpha \sqrt{1 - \cos\psi}\, d\psi = 8\sqrt{\tilde{\sigma}}[1 - \cos(\alpha/2)]. \tag{9}$$

For the part of the membrane adhered to the cylinder, the free energy consists of two parts. The adhesion energy, proportional to the surface area of the adhered membrane is

$$E_{\mathrm{ad}} = -w2RL\alpha. \tag{10}$$

Introducing a rescaled adhesion energy per unit area

$$\tilde{w} = \frac{wR^2}{\kappa}, \tag{11}$$

the reduced adhesion energy $\tilde{E}_{\mathrm{ad}} = E_{\mathrm{ad}}R/\kappa L$ can then be written as

$$\tilde{E}_{\mathrm{ad}} = -2\tilde{w}\alpha. \tag{12}$$

The second part is the membrane free energy [Eq. (5)] in the contact area, where we have $d\psi/d\tilde{s} = \alpha/(R\alpha/R) = 1$. The integration in Eq. (5) gives,

$$\Delta F_{\mathrm{contact}} = 2\alpha + 2\tilde{\sigma}(\alpha - \sin\alpha). \tag{13}$$

Taking into account the above adhesion energy of the contact portion and the contributions from two free portions of the membrane, to the left and right sides of the cylinder, for the entire system we have

$$\begin{aligned}\Delta\tilde{F}_I &= \Delta\tilde{F}_{\mathrm{free}} + \tilde{E}_{\mathrm{ad}} + \Delta\tilde{F}_{\mathrm{contact}} \\ &= 8\sqrt{\tilde{\sigma}}[1 - \cos(\alpha/2)] - (2\tilde{w} - 1)\alpha + 2\tilde{\sigma}(\alpha - \sin\alpha).\end{aligned} \tag{14}$$

At this stage, in order to make a comparison with a typical Ginzburg-Landau theory in phase transitions, we can make a small-α expansion of $\Delta\tilde{F}_I$, which leads to

$$\Delta\tilde{F}_I = (1 - 2\tilde{w})\alpha + \sqrt{\tilde{\sigma}}\alpha^2 + \cdots. \tag{15}$$

One can then conclude that a second-order phase transition takes place as $1-2\tilde{w}=0$ for any $\tilde{\sigma}$ and that the relevant "order parameter" in the theory is the square root wrapping angle, $\sqrt{\alpha}$. Figure 2(A) is the resulting phase diagram from an analysis of the above free energy. For any values of $\tilde{\sigma}$, in the region $\tilde{w} \leq 1/2$, the cylinder is in a free, desorbed state; in the region where $\tilde{w}$ is somewhat larger than 1/2, the system contains a membrane weakly wrapping around the cylinder. The same conclusion about the transition was drawn earlier in Ref. [28], where it was shown that a two-dimensional bead with the radius $R \leq (\kappa/2w)^{\frac{1}{2}}$ does not adhere to a flat membrane.

In the adsorbed region $\tilde{w} \geq 1/2$, without using a small-α expansion, we can directly minimize Eq. (14) with respect to the wrapping angle α. This procedure yields a preferred cosine wrapping angle as a function of $\tilde{w}$ and $\tilde{\sigma}$,

$$\cos\alpha = 1 - [(2\tilde{w})^{1/2} - 1]^2/(2\tilde{\sigma}). \tag{16}$$

Using the scaling factors in Ref. [21], we can show that the above expression agrees exactly with formulas (46) and (48) in Ref. [21]. For a given adhesion energy $\tilde{w}$, as $\tilde{\sigma}$ is reduced the membrane wraps the cylinder more deeply with a larger wrapping angle α.

The minimal distance between the two portions of the wrapping membrane, one on the left and the other on the right [Fig. 2(C)], can be written as $D_{\mathrm{mem}} = \tilde{D}_{\mathrm{mem}}R$, where

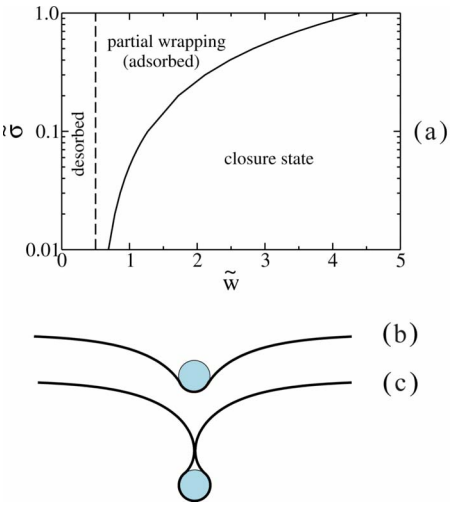

FIG. 2. (Color online) Adhesion of a single cylinder to a membrane. The phase diagram for the system of a cylinder adhering to a membrane as a function of the reduced surface tension and adhesion energy is shown in plot (a). The illustrations in (b) and (c) are sketches for a typical partial wrapping state and typical closure state, respectively.

$$\begin{aligned}\tilde{D}_{\mathrm{mem}} &= 2\sin\alpha - 2\int_0^{\tilde{s}'} \cos\psi d\tilde{s} \\ &= 2\sin\alpha + \frac{2}{\sqrt{2\tilde{\sigma}}}\int_{\pi/2}^{\alpha} \frac{\cos\psi}{\sqrt{1-\cos\psi}} d\psi \\ &= \sin\alpha + \frac{1}{\sqrt{\tilde{\sigma}}}\left[\ln\frac{\tan\frac{\alpha}{4}}{\tan\frac{\pi}{8}} + 2\left(\cos\frac{\alpha}{2} - \cos\frac{\pi}{4}\right)\right],\end{aligned} \tag{17}$$

where $\psi(\tilde{s}') = \pi/2$. In this expression the second term represents the horizontal distance that the free membrane portion makes, starting from the contact point with the cylinder to the contact point of the membrane from the other side. In terms of $\tilde{w}$ and $\tilde{\sigma}$ the closure condition can be deduced from joint consideration of Eq. (16) and the requirement $\tilde{D}_{\mathrm{mem}} = 0$. Numerically eliminating α from (16) and (17) we obtain the solid contact line in Fig. 2(A).

Considering the problem of adhesion of a single *spherical* colloid to a membrane surface, Deserno [13,14] previously obtained a phase diagram qualitatively similar to ours in Fig. 2(A). The transition from the free to partial wrapping phase, for example, is also a second-order transition but at a different location because of the spherical symmetry. Furthermore, Deserno has defined a fully enveloping state where the wrapping angle in his system, similar to our α in this paper, jumps to a large value near π. The transition from the partial wrapping to enveloping states was shown to be first order by examination of the free energy; in contrast, in the case of

cylinder adhesion, we did not find that such a transition is of a phase-transition nature; the transition from partial wrapping to closure states is a smooth crossover with no signature of a typical phase transition, by an examination of the free energy in this work.

Note that in most natural membrane systems, $\kappa \simeq 20k_BT$ which is much greater than typical energy fluctuations, of order k_BT, in the system. This ensures that thermal fluctuations about the free energy minimum found here can be neglected in most regions of the parameter space. Within this approximation, the κ dependence of the phase boundaries in Fig. 2(C) enters only through $\tilde{\sigma}$ and $\tilde{w}$ [see Eqs. (3) and (11)]. However, there are regions in the parameter space, such as near the second-order transition line discussed above and also second order transition points presented in the next two sections, where thermal fluctuations become important; the phase boundaries based on the current treatment may alter near these places while the qualitative phase behavior remains the same.

IV. ADHESION OF TWO CYLINDERS TO THE SAME SIDE OF A MEMBRANE

In this section we examine the problem of adhesion of two parallel cylinders to the same side of a membrane, where the surface-to-surface distance of two parallel cylinders is fixed at D, as illustrated in Fig. 1(B). In this system the free energy can be separated into two parts

$$\Delta\tilde{F}_{II}(\alpha,\gamma,\zeta) = \Delta\tilde{F}_I(\alpha) + \Delta\tilde{F}'_I(\gamma,\zeta), \tag{18}$$

where $\Delta\tilde{F}_I(\alpha)$ is the summed free energy of the two portions of the system, to the left side of the vertical diameter of the left cylinder and the right side of the vertical diameter of the right cylinder, shown in Fig. 1(B), and $\Delta\tilde{F}'_I(\gamma,\zeta)$ is the free energy of the middle portion between the two vertical lines.

The membrane shape in the middle portion can also be described by the shape equation, Eq. (7). We select the symmetric point in the middle as the reference point to determine the integration constant H in Eq. (7); at this point $\psi=0$ but the curvature $d\psi/ds=\zeta$ is not. Here we use ζ as an unknown free parameter, to be determined below, and write $H=\zeta^2/2$. Then

$$\left(\frac{d\psi}{d\tilde{s}}\right)^2 = \zeta^2 + 2\tilde{\sigma}(1-\cos\psi). \tag{19}$$

Taking into account the adhesion energy of the contact portion and converting the integration over $\tilde{s}$ in Eq. (5) to integration over ψ, we have

$$\Delta\tilde{F}'_I(\gamma,\zeta) = \int_0^\gamma \frac{\zeta^2 + 4\tilde{\sigma}(1-\cos\psi)}{\sqrt{\zeta^2 + 2\tilde{\sigma}(1-\cos\psi)}}d\psi - (2\tilde{w}-1)\gamma + 2\tilde{\sigma}(\gamma - \sin\gamma), \tag{20}$$

where γ is the wrapping angle shown in Fig. 1(B). The reduced distance between the surfaces of two cylinders can be written by the use of the shape function

$$\tilde{D} = \int_0^{\tilde{s}''} \cos\psi d\tilde{s} + 2\sin\gamma - 2, \tag{21}$$

where $\tilde{s}''$ is the location of the middle point between two cylinders. Changing the variable to ψ using Eq. (19), we have

$$\tilde{D}(\gamma,\zeta) = \int_0^\gamma \frac{2\cos\psi}{\sqrt{\zeta^2 + 2\tilde{\sigma}(1-\cos\psi)}}d\psi + 2(\sin\gamma - 1). \tag{22}$$

The integrals in Eqs. (20) and (22) can be expressed by elliptic integrals of the first and second kinds. Instead of these special functions, below we use the original integration forms in carrying out the numerical computation.

The minimization of the free energy of the entire system, $\Delta\tilde{F}_{II}(\alpha,\gamma,\zeta)$, with respect to three parameters, α, γ, and ζ, can be formulated in two separate steps. Because α only appears in one of the two additive terms in Eq. (18) and $\tilde{D}$ is independent of α, the two contributions in Eq. (18) can be treated independently. The minimization of $\Delta\tilde{F}_I(\alpha)$ gives exactly the same condition for the wrapping angle α in Eq. (16), which can be substituted into Eq. (14) for the calculation of the free energy minimum.

One can, for example, implement an undetermined Lagrangian multiplier method and make use of constraint (22). In our numerical treatment, we adopt a simple look-up table method for the two-variable functions in Eqs. (20) and (22). These functions are numerically computed at small increments of γ and ζ, and when a given $\tilde{\sigma}$ is specified, a data table for the first term in Eq. (20) for $\Delta\tilde{F}'_I$ and the entire right-hand side in Eq. (22) for $\tilde{D}$ is created. With a given value of $\tilde{D}$, a search for the minimum value of $\Delta\tilde{F}'_I$, which now contains the other terms in Eq. (20) as well, can then be numerically performed by going through this look-up table. This way, we can determine the location (i.e., the values of γ and ζ) of the minimum of $\Delta\tilde{F}'_I$, by prespecified $\tilde{w}$, $\tilde{D}$, and $\tilde{\sigma}$. The numerical table was refined to achieve the desired numerical precision after an initial search.

The resulting energy minimum, $\Delta\tilde{F}'_I$, is displayed as a function of $\tilde{D}$ for various values of $\tilde{\sigma}$ and $\tilde{w}$ in Figs. 3(A)–3(C). The free energy has two branches in some parameter region, corresponding to two typical membrane shapes between the cylinders. In relatively small $\tilde{w}$ and large $\tilde{\sigma}$ regime, the membrane wraps two cylinders with a shallow shape, shown in Fig. 3(D). The solid curves in Figs. 3(A)–3(C) are produced from such configurations. In the region of relatively large $\tilde{w}$ and small $\tilde{\sigma}$, deep membrane wrapping can develop [Fig. 3(E)] between the cylinders, which has a lower intermembrane free energy in comparison with that of the shallow shape. The dashed curves in Figs. 3(A)–3(C) are produced from deep configurations. Taking the curve of $\tilde{w}=1.1$ and $\tilde{\sigma}=0.1$ in Fig. 3(B), for example, by increasing $\tilde{D}$, we see a first-order transition approximately at $\tilde{D}=2.0$, signified by the crossing of the two branches of the free energy; as $\tilde{D}$ moves across the transition point, the shal-

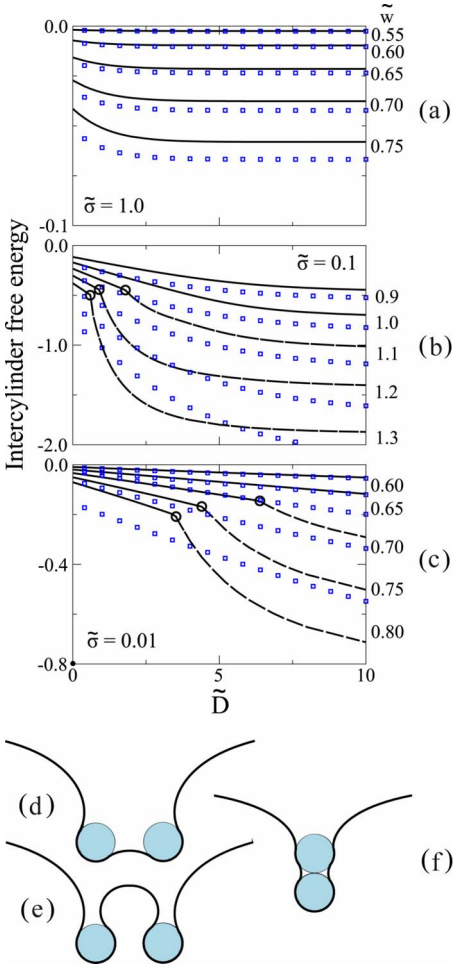

FIG. 3. (Color online) Adhesion of two cylinders to the same side of a membrane. The intercylinder free energy difference, $\Delta\tilde{F}_I'$ in Eq. (20), as a function of the surface-to-surface distance between the cylinders, $\tilde{D}$, is shown in plots (a)–(c) for $\tilde{\sigma}=1.0$, 0.1, and 0.01. Two branches of the free energy are shown using solid and long-dashed curves. Squares represent the results from a perturbation theory in Ref. [20]. Circles represent the locations where two branches cross, hence the locations of first-order transitions. Sketches (d)–(f) are three typical configurations of the system.

low wrapping of the intercylinder membrane on the cylinders [Fig. 3(D)] abruptly jumps to deep wrapping [Fig. 3(E)]. This transition is driven by the adhesion energy that prefers a more complete wrapping of membrane on the cylinders and is unfavored by the membrane free energy that prefers a smooth variation of the shape function. In general, for systems with large $\tilde{\sigma}$, the membrane free energy dominates hence we see that the shallow shapes are more stable.

From a different perspective, we can view the stable regions of the shallow and deep phases in a phase diagram shown in Fig. 4 for a given value of $\tilde{w}$. The shallow conformation is stable in the region to the low-right corner of a solid first-order phase transition line and the deep conformation is stable in the left-upper corner of the line. In a typical experimental setup the transition can be accessed by either varying $\tilde{D}$ or $\tilde{\sigma}$ in the system. The first-order transition terminates at a second-order point represented by a square;

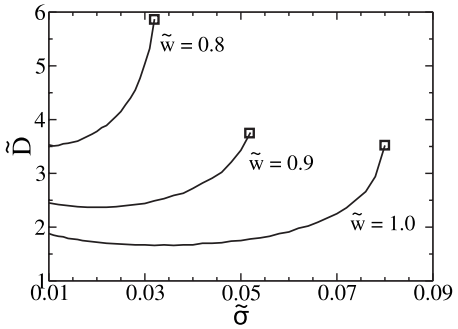

FIG. 4. Phase diagrams of the shallow-to-deep phase transition for $\tilde{w}=0.8$, $\tilde{w}=0.9$, and $\tilde{w}=1.0$ as a function of surface-to-surface distance $\tilde{D}$ and reduced tension $\tilde{\sigma}$. The area below a solid transition line corresponds to the shallow configuration, and the area above a transition line corresponds to deep wrapping. First-order transition solid lines terminate at a second-order point specified by a square on the plots.

above the critical $\tilde{D}$ value, the crossover between the shallow and deep profiles is smooth.

Take the system of $\tilde{\sigma}=0.1$ and $\tilde{w}=1.069$ for example, where a first-order transition takes place at $\tilde{D}=3.0$. At three separate values of $\tilde{D}$ in Fig. 5(A) we have plotted the intercylinder free energy as a function of the wrapping angle γ to demonstrate the first-order transition. At $\tilde{D}=1.8$ below the transition, the free energy has a minimum at a small wrapping angle corresponding to a shallow configuration, where another higher free energy minimum is visible at a larger wrapping angle. At $\tilde{D}=4.1$ above the transition, the free energy minimum at the larger wrapping angle has a lower value than that at the small wrapping. The energy barrier between the shallow- and deep-wrapping configurations can also be viewed from Fig. 5(A). Typically, at small values of $\tilde{D}$ the energy barrier is high hence the shallow configuration is relatively stable; whereas at large values of $\tilde{D}$ the energy barrier is low hence the tunneling between the shallow and deep wrapping can take place relatively easily.

Take another system of $\tilde{\sigma}=0.1$ and $\tilde{w}=1.1$ for example, where a first-order transition takes place at $\tilde{D}=1.84$. Again, at three different values of $\tilde{D}$, in Fig. 5(B) we have plotted the intercylinder free energy as a function of the wrapping angle γ. Most features described in the previous paragraph remain the same, however, with one difference. The region represented by the shaded area in Fig. 5(B) corresponds to a closure state where the membrane shape near each of the two cylinders displays a configuration shown in Fig. 2(C). The shallow-to-deep first-order transition then becomes a shallow-to-closure first-order transition.

Regardless of the fact that system is in shallow or deep configuration, as $\tilde{D}$ increases the intercylinder free energy $\Delta\tilde{F}_I'$ generally decreases. Hence, for the problem of two cylinders adhering to the same side of a membrane surface, there is a membrane-mediated repulsion between the two cylinders. This conclusion has been previously drawn by Weikl [20] who took a small-displacement expansion of the

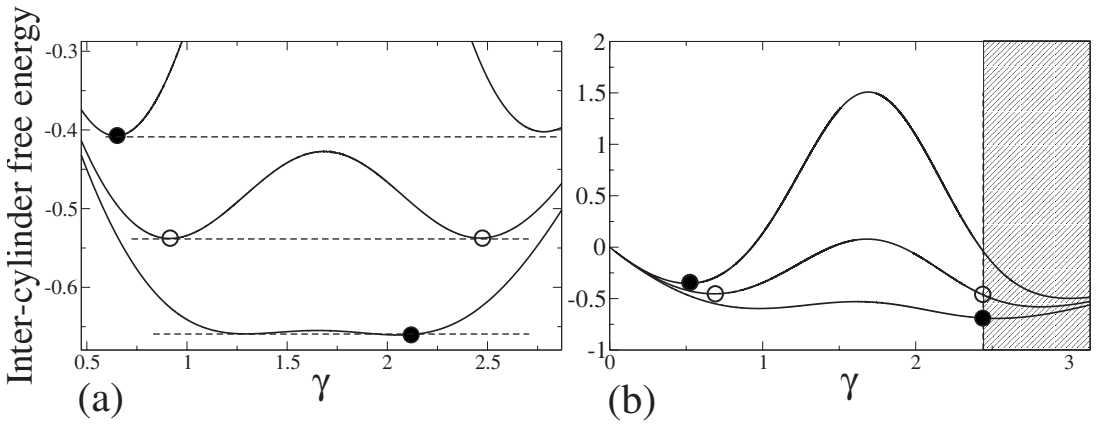

FIG. 5. Dependence of the intercylinder free energy [in Eq. (20)] on the wrapping angle γ, when the distance between the adhered cylinders is fixed. (a) The free energy is plotted for $\tilde{\sigma}=0.1$, $\tilde{w}=1.069$, and $\tilde{D}=1.8,3.0,4.1$ from top to bottom. (b) The free energy is plotted for $\tilde{\sigma}=0.1$, $\tilde{w}=1.1$, and $\tilde{D}=1.0,1.84,3.0$ from top to bottom. The open circles denote double energy minima, and solid circles single energy minimum. The shaded area in (b) corresponds to the closure state.

Helfrich free energy as the starting point. In such an approximation, only shallow intercylinder membrane configurations can be captured. We overlayed Weikl's estimation of the free energy in Figs. 3(A)–3(C) using open squares, for every set of numerical solutions obtained in our calculation. The comparison between our full calculation and Weikl's approximation is favorable for $\tilde{w}$ close to the free-to-partial wrapping transition, where a small degree of wrapping is generally expected.

The possible existence of shallow and deep profiles for a given $\tilde{D}$ was discussed in Ref. [21] as well, where both profiles are shown stable in a small $\tilde{D}$ region. Instead of directly minimizing the free energy for a given $\tilde{w}$, Ref. [21] considers the balance of torque in the system, and focuses on a case where the total wrapping angle, $\gamma+\alpha$, is kept constant. Note that the two profiles produced this way correspond to stable profiles in our work at two different values of $\tilde{w}$. There is a one-to-one mapping between a given $\tilde{w}$ and a given value of angle $\gamma+\alpha$, for each branch of the free energy. Although the perspectives are different, the conclusions on the existence of shallow and deep profiles below a critical $\tilde{D}$ are the same.

The interplay between shallow and deep shapes of membrane between two colloid particles has also recently been seen in another system; when two spherical particles are confined in a cylindrical membrane tube [22], Chen, Liu, and Liang showed that this interplay can manifest into a more sophisticated phase diagram, where both attraction and repulsion between two spheres can be mediated by the wrapping membrane.

As a final note, we have also considered the configuration where one cylinder vertically stacks on the other [see Fig. 3(F)]. The free energy can be numerically calculated in a similar way but cares must be taken in setting the correct free energy zero for the intercylinder portion of the membrane in order to compare it with that of other conformations. In the entire parameter regime studied here, $\tilde{w}=[1/2,10]$ and $\tilde{\sigma}=[0.01,1]$, we found no evidence that this type of configurations may have lower free energy than the free energy corresponding to two parallel cylinders separated far apart, each adhering to the membrane independently, which was considered above.

V. ADHESION OF TWO CYLINDERS TO OPPOSITE SIDES OF A MEMBRANE

In this section, we consider the adhesion of two cylinders to opposite sides of a membrane [see Fig. 1(C)], a system that was initially discussed in Ref. [20]. In particular, we assume that the membrane has a dimension larger than the length of the cylinders and the left and right boundaries of the membrane reach a flat shape in infinity at an equal height. The coordinate system is shown in Fig. 1(C), where the system configuration is antisymmetric with respect to the center. The free energy of the system can also be separated into two contributions,

$$\Delta\tilde{F}_{II}(\alpha,\gamma,\theta)=\Delta\tilde{F}_{I}(\alpha)+\Delta\tilde{F}'_{I}(\gamma,\theta). \tag{23}$$

Again, $\Delta\tilde{F}'_{I}(\gamma,\theta)$ represents the free energy of the system between two vertical diameter lines in Fig. 1(C) and $\Delta\tilde{F}_{I}(\alpha)$ the rest of the system. The latter has the same form as that for a single cylinder adhesion problem, Eq. (14). Using the coordinate system in Fig. 1(C), we see that at the middle point of the stretched membrane between two cylinders, the curve makes an angle θ with respect to the horizontal axis, while the curvature vanishes because of the antisymmetry; this fact gives us an integration constant $H=-\tilde{\sigma}(1-\cos\theta)$ in Eq. (7). We then have

$$\frac{1}{2}\left(\frac{d\psi}{d\tilde{s}}\right)^2-\tilde{\sigma}(1-\cos\psi)=-\tilde{\sigma}(1-\cos\theta). \tag{24}$$

Using $d\psi/d\tilde{s}$ from this equation and taking the adhesion energy into account, we obtain

$$\Delta\tilde{F}'_{I}(\gamma,\theta)=\sqrt{2\tilde{\sigma}}\int_{\theta}^{\gamma}\frac{\cos\theta-2\cos\psi+1}{\sqrt{\cos\theta-\cos\psi}}d\psi-(2\tilde{w}-1)\gamma$$
$$+2\tilde{\sigma}(\gamma-\sin\gamma), \tag{25}$$

where γ is the wrapping angle shown in Fig. 1(C).

Measured from the center, two cylinders have the same height h to the membrane plane, which defines a constraint on the parameters of the system. Using the shape function in Sec. III, we can determine the reduced height,

$$\tilde{h}(\alpha) \equiv h/R = \frac{1}{\sqrt{2\tilde{\sigma}}}\int_0^{\alpha} \frac{\sin\psi}{\sqrt{1-\cos\psi}}d\psi - \cos\alpha$$

$$= \frac{2}{\sqrt{\tilde{\sigma}}}\sin(\alpha/2) - \cos\alpha, \tag{26}$$

where α is the optimal wrapping angle in Eq. (16) that minimizes the free energy Eq. (14). On the other hand, the configuration of the intercylinder membrane can also be solved by using the shape equation but now with parameters γ and θ as boundary conditions. The same height can be written as

$$\tilde{h}(\gamma,\theta) = \frac{1}{\sqrt{2\tilde{\sigma}}}\int_{\theta}^{\gamma} \frac{\sin\psi}{\sqrt{\cos\theta-\cos\psi}}d\psi - \cos\gamma$$

$$= \sqrt{\frac{2}{\tilde{\sigma}}}\sqrt{\cos\theta-\cos\gamma} - \cos\gamma. \tag{27}$$

Equating these two expressions, Eqs. (26) and (27), gives rise to a constraint that governs a relationship between the three angular parameters α, γ, and θ. While α can be determined separately, given by Eq. (16), the constraint produces a relationship between two parameters, γ and θ, only one of which is independent at this stage.

To study the membrane-mediated interaction between the two adsorbed cylinders, in the following we are interested in the free energy as a function of the reduced distance $\tilde{D}$, which can be expressed as a function of γ,θ as well,

$$\tilde{D}(\gamma,\theta) = \sqrt{\frac{2}{\tilde{\sigma}}}\int_{\theta}^{\gamma} \frac{\cos\psi}{\sqrt{\cos\theta-\cos\psi}}d\psi + 2(\sin\gamma - 1). \tag{28}$$

Once $\tilde{D}$ is given, this adds another constraint on the parameter γ and θ; therefore, in a system with fixed $\tilde{D}$, all three angular parameters, α, γ and θ, are completely determined.

The resulting free energy for the system, $\Delta\tilde{F}_{II}$, as a function of $\tilde{D}$, is displayed in Figs. 6(A)–6(C) for various sets of $\tilde{w}$ and $\tilde{\sigma}$. When both cylinders are weakly adsorbed, a typical free energy curve [for example, the curve labeled $\tilde{w}=1.25$ in Fig. 6(A) or $\tilde{w}=0.60$ in Fig. 6(B)] contains a minimum somewhat below $\tilde{D}=0$; this usually happens for small $\tilde{w}$ where two cylinders prefer to be in a shallowly wrapped configuration shown in Fig. 6(D), at the free energy minimum. The total free energy is dominated by the contribution from the free energy cost of distorting the membrane shape.

In a large $\tilde{w}$ region, however, the adhesion energy prefers having a large wrapping area between cylinders and the wrapping membrane, in expense of creating a large membrane shape distortion unwanted by the membrane energy. A typical configuration of this type is shown in Fig. 6(E), where, because of the swapping of the positions of two cylinders, the surface distance defined in Fig. 1(C) reaches a value close to −4.

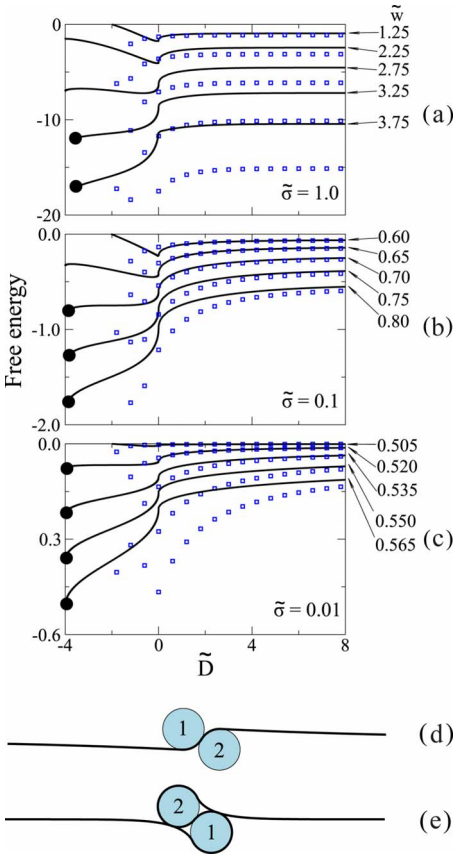

FIG. 6. (Color online) Adhesion of two parallel cylinders to opposite sides of a membrane. Plots (a), (b), and (c) show the free energy dependence [Eq. (23) after minimization] on the surface-to-surface distance $\tilde{D}$ between the cylinders for a several given sets of $\tilde{w}$ and $\tilde{\sigma}$. The location of a terminal minimum near $\tilde{D}=-4$ is also shown by a circle. Overlaying on the curves are squares, which represent the results calculated from Ref. [20], agreeing well with our results in weak adhesion. The configuration in (d) is a sketch of a typical shallow adsorption profile and the configuration in (e) is a sketch for a typical wrapping state where the positions of the cylinders are exchanged from those in (d).

The development of a minimum in the free energy curve near $\tilde{D}=-4$ can be viewed in Figs. 6(A) and 6(B) in a series of curves corresponding to increasing $\tilde{w}$. Note that the free energy curve has a termination point where the system is in a full wrapping state, which is a case where two cylinders touch the membrane from opposite sides after the exchange of the positions; we indicate such a closure state by filled circles in Figs. 6(A)–6(C). A first-order swapping phase transition from a partial wrapping state [Fig. 6(D)] to a closure state [Fig. 6(E)] takes place as the new free energy minimum becomes deeper. In Fig. 7, we display a phase diagram where the solid line displays the location of the swapping transition between these two states.

The free energy in Fig. 6 has minima in low values of $\tilde{D}$ only. This means that in the entire parameter space considered here, the two oppositely adhered cylinders experience a membrane-mediated attraction, which prefers a small separation between the two. Two cylinders reach a close contact

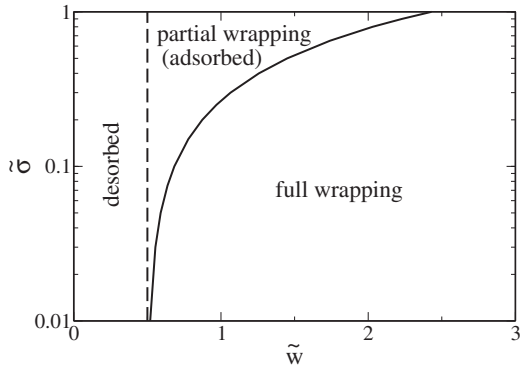

FIG. 7. Phase diagram of the system where two cylinders adhere to opposite sides of a membrane. The dashed line represents the same second-order adsorption transition shown in Fig. 2(A) and the solid curve represents a first-order swapping transition, where the system undergoes a transition from a state with the membrane weakly wrapping two parallel cylinders [plot (d) in Fig. 6] to a state with the membrane fully wrapping both cylinders (the positions of cylinders are exchanged in the horizontal direction [plot (e) in Fig. 6]).

with the membrane in between, by a distance limited by the excluded volume between cylinders. The conclusion of a membrane-mediated attraction between two oppositely adhered cylinders was previously suggested by Weikl, who considered a small-displacement expansion of the Helfrich model [20] and concluded in a recent publication as well [21]. In Figs. 6(A)–6(C), we replot Weikl's approximation for the free energy by open squares for comparison; unsurprisingly, in weak adsorption, our full solution and Weikl's approximation overlap on each other.

The model described in this section is suitable for adhesion of two parallel cylinders to a much larger membrane surface, which can be compared with the adhesion problem of two parallel cylinders to a membrane that has a relatively smaller dimension (shorter than the cylinder height) along the axial direction of the cylinder; in the latter system the adhesion of two cylinders to the opposite sides of the membrane breaks the same-height requirement used above—a case that has been recently noted in Ref. [21]. While the two systems are somewhat different, the conclusion that the two oppositely adhered cylinders always experience membrane-mediated attraction is in common.

VI. SUMMARY

In summary, on the basis of a full treatment of the Helfrich model, we have shown that deep wrapping of a membrane on cylinders can cause significant structural behavior that is much richer than those obtained from a small-displacement approximation [20]. The main results here are obtained from an analysis of the free energy and are fully consistent with a recent consideration of same systems from an analysis of force involved in the system [21]. In the case of two parallel cylinders adhering to the same side of a membrane, a new branch of the free energy function, which was not considered previously in Ref. [20] but suggested in Ref. [21], has been calculated. In the case of two parallel cylinders adhering to opposite sides of a membrane, the free energy minimum of the system corresponds to a conformation where two cylinders are in contact; furthermore, a first-order swapping phase transition from shallow to full wrapping of the membrane on the cylinders is shown to exist in some region of the parameter space.

ACKNOWLEDGMENTS

We thank Natural Science and Engineering Research Council of Canada for financial support and SHARCNET for providing computational time.

[1] C. Hiergeist, V. A. Indrani, and R. Lipowsky, Europhys. Lett. **36**, 491 (1996).
[2] K. Yaman, P. Pincus, and C. M. Marques, Phys. Rev. Lett. **78**, 4514 (1997).
[3] Y. W. Kim and W. Sung, Europhys. Lett. **47**, 292 (1999).
[4] M. Breidenich, R. R. Netz, and R. Lipowsky, Europhys. Lett. **49**, 431 (2000).
[5] M. Breidenich, R. R. Netz, and R. Lipowsky, Eur. Phys. J. E **5**, 403 (2001).
[6] Y. W. Kim and W. Sung, Phys. Rev. E **63**, 041910 (2001).
[7] M. Laradji, Europhys. Lett. **60**, 594 (2002).
[8] M. Laradji, J. Chem. Phys. **121**, 1591 (2004).
[9] T. Auth and G. Gompper, Phys. Rev. E **72**, 031904 (2005).
[10] R. Lipowsky and H.-G. Dobereiner, Europhys. Lett. **43**, 219 (1998).
[11] T. Bickel, J. Chem. Phys. **118**, 8960 (2003).
[12] B. Rozycki, R. Lipowsky, and T. R. Weikl, Europhys. Lett. **84**, 26004 (2008).
[13] M. Deserno, Phys. Rev. E **69**, 031903 (2004).
[14] M. Deserno, J. Phys.: Condens. Matter **16**, S2061 (2004).
[15] H. Noguchi and M. Takasu, Biophys. J. **83**, 299 (2002).
[16] Y. Li, X. Chen, and N. Gu, J. Phys. Chem. B **112**, 16647 (2008).
[17] I. Tsafrir, D. Sagi, T. Arzi, M.-A. Guedeau-Boudeville, V. Frette, D. Kandel, and J. Stavans, Phys. Rev. Lett. **86**, 1138 (2001).
[18] F. Brochard-Wyart, T. Tanaka, N. Borghi, and P.-G. de Gennes, Langmuir **21**, 4144 (2005).
[19] J. Z. Y. Chen, Phys. Rev. Lett. **98**, 088302 (2007).
[20] T. R. Weikl, Eur. Phys. J. E **12**, 265 (2003).
[21] M. M. Muller, M. Deserno, and J. Guven, Phys. Rev. E **76**, 011921 (2007).
[22] J. Z. Y. Chen, Y. Liu, and H. J. Liang, Phys. Rev. Lett. **102**, 168103 (2009).
[23] W. Helfrich and R. M. Servuss, Nuovo Cimento D **3**, 137 (1984).
[24] W. Helfrich, Z. Naturforsch. C **28**, 693 (1973).
[25] U. Seifert, Adv. Phys. **46**, 13 (1997).

[26] M. Muller, K. Katsov, and M. Schick, Phys. Rep. **434**, 113 (2006).
[27] M. Deserno and T. Bickel, Europhys. Lett. **62**, 767 (2003).
[28] A. Boulbitch, Europhys. Lett. **59**, 910 (2002).
[29] M. M. Muller, M. Deserno, and J. Guven, Europhys. Lett. **69**, 482 (2005).
[30] K. Takei, V. I. Slepnev, V. Haucke, and P. De Camilli, Nat. Cell Biol. **1**, 33 (1999).
[31] Q. Wang, M. V. A. S. Navarro, G. Peng, E. Molinelli, S. L. Goh, B. L. Judson, K. R. Rajashankar, and H. Sondermann, Proc. Natl. Acad. Sci. U.S.A. **106**, 12700 (2009).